Side Lobe Suppression of Marine-Radar Linear Array Antenna by a Reflectionless Metasurface

Y. Kato[1,2], Y. She[1], S. Kurokawa[1], and A. Sanada[2]
[1]Research Institute for Physical Measurement, National Institute of Advanced Industrial Science and Technology
1-1-1 Umezono, Tsukuba, Ibaraki 305-8568, Japan
[2]Gradual School of Engineering Science, Osaka University
1-3 Machikaneyama, Toyonaka, Osaka 560-8531, Japan

***Abstract*-This paper demonstrates a side lobe suppression technique of a marine radar linear slot array antenna by a reflectionless metasurface. The metasurface introduces position-dependent phase shifts so that the phase across the entire aperture can be uniform. It is numerically shown that the metasurface drastically suppresses the maximum side lobe level at 9.41 GHz to be below –24 dB in both the E and H planes, and as a consequence, the peak gain of the main lobe is increased by 1.4 dB.**

I. Introduction

High-gain array antennas are required for marine radar applications. In the radar applications, side lobe suppression is a key issue as well as gain enhancement of the main lobe. In the conventional array antennas with baffle plates [1], for instance, there exists a phase shift near the edge of the aperture compared with that near the center, which leads to the side lobe generations [2]. Generally speaking, it is difficult to control the phase over the entire aperture especially in the linear array antennas.

In this paper, we propose a side lobe suppression technique for a linear slot array antenna by using a reflectionless metasurface for marine radar applications. The metasurface placed in front of the slot array provides the phase of the radiation fields to be uniform across the aperture. By compensating the phase deviation near the aperture edge, the side lobe suppression can be achieved. We design a tri-layer metasurface for the radiation fields' phase control of a slot array antenna with the aperture size of 600 mm × 100 mm at 9.41 GHz for marine radar applications and numerically demonstrate its performance by full-wave simulations.

II. Antenna and Metasurface Design

A. Slot array antenna

Fig. 1 shows the antenna system studied in this paper. The antenna consists of a transverse slot linear array antenna proposed for marine radar applications [1] and a metasurface covering the antenna aperture. The slot linear array uses a quasi-TEM mode waveguide consisting of a WR-90 rectangular waveguide partially filled with dielectrics on the narrow side walls and radiates the linearly polarized beam in the *y*-direction with a low cross-polarization. Two metal baffle plates in the horn shape are introduced to increase the gain. The aperture dimensions are 600 mm × 100 mm. Please refer to [1] for more details on the antenna design.

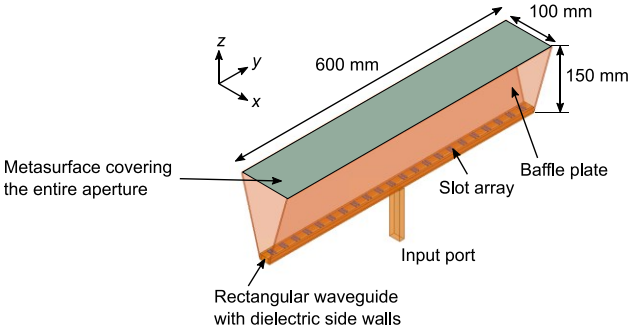

Figure 1. Slot array antenna with a metasurface covering the entire aperture.

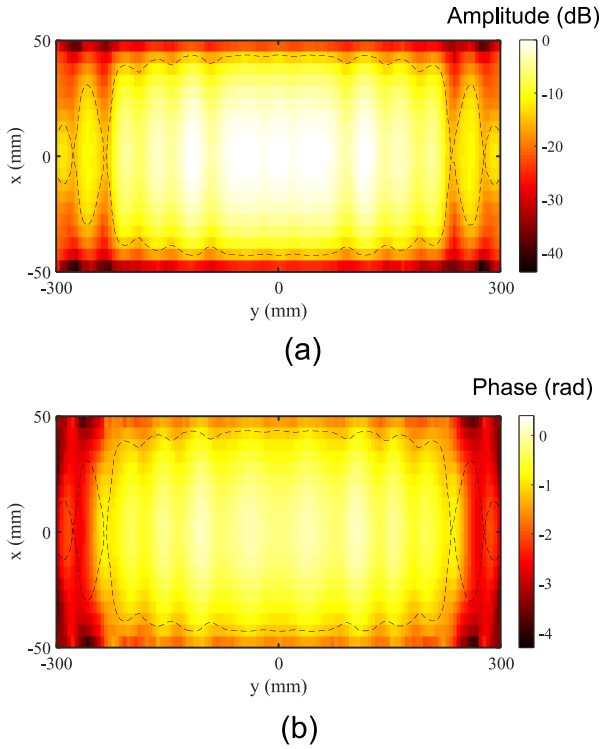

Figure 2. (a) Amplitude and (b) phase of the electric-field distributions on the entire aperture of the slot array antenna.

Fig. 2 shows the amplitude and phase of the simulated electric-field distributions on the aperture parallel to the *zx*-plane at 9.41 GHz obtained from full-wave simulations using the HFSS driven solver. As can be seen from Fig. 2(b), the

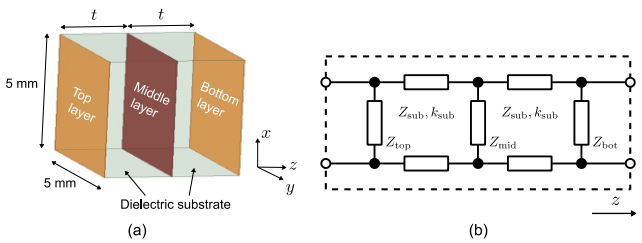

Figure 3. (a) Schematic drawing and (b) equivalent circuit of the unit cell of the tri-layer metasurface.

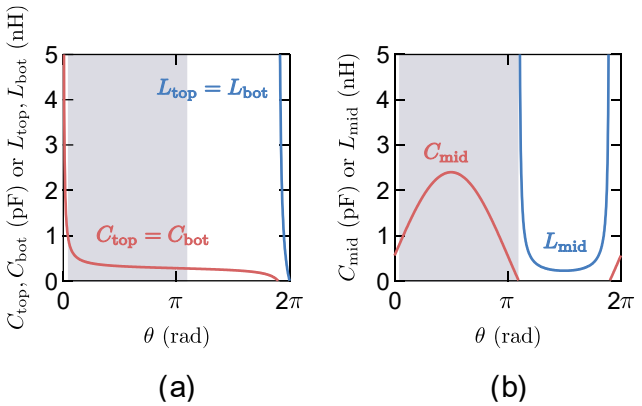

Figure 4. Capacitance or inductance values of (a) the top/bottom and (b) middle layers corresponding to the phase shift of θ.

phase changes from the center to the edge of the aperture. The dashed lines in the figure indicate the contour with the amplitude of –15 dB. Within the region where the amplitude is greater than –15 dB, the maximum phase variation is 2.88 rad. This phase nonuniformity leads to high level side lobe.

B. Metasurface

To compensate the phase variations in Fig. 2(b), the entire aperture is covered by the metasurface that is designed as follows. First, the aperture area is divided into cells with the size of 5 mm × 5 mm (Number of cells: 20 × 120). The metasurface introduces a position-dependent phase shift to an incident wave without reflections. The local S-parameters of each unit cell are given by

$$[S] = \begin{pmatrix} 0 & \exp(j\theta) \\ \exp(j\theta) & 0 \end{pmatrix}, \tag{1}$$

where θ is a phase shift. The local Z-parameters are calculated from (1) as

$$[Z] = Z_0 \begin{pmatrix} \frac{1+e^{2j\theta}}{1-e^{2j\theta}} & \frac{2e^{2j\theta}}{1-e^{2j\theta}} \\ \frac{2e^{2j\theta}}{1-e^{2j\theta}} & \frac{1+e^{2j\theta}}{1-e^{2j\theta}} \end{pmatrix}, \tag{2}$$

where Z_0 is the free space impedance. Z-parameters of the cells for the required phase transformations are implemented by a tri-layer metasurface [3] whose unit cell is shown in Fig. 3(a). The equivalent circuit for the unit cell is shown in Fig. 3(b), where Z_{top}, Z_{mid}, and Z_{bot} are the shunt impedance of the top, middle, and bottom layers, respectively. The dielectric substrates with the relative permittivity ϵ_r are expressed as transmission lines with the wave impedance $Z_{\text{sub}} = Z_0/\sqrt{\epsilon_r}$ and wavenumber $k_{\text{sub}} = \sqrt{\epsilon_r}\, k_0$, where k_0 is the free space wavenumber. According to the transmission line theory, the shunt impedances for realizing the Z-parameters of (2) are given by [4]

$$Z_{\text{top}} = Z_{\text{bot}} = -j\left(\frac{\cot k_{\text{sub}} t}{Z_{\text{sub}}} + \frac{1+\cos\theta}{\sin\theta}\frac{1}{Z_0}\right)^{-1},$$
$$Z_{\text{mid}} = -j\frac{Z_{\text{sub}}^2 \sin^2 k_{\text{sub}} t}{Z_{\text{sub}} \sin 2k_{\text{sub}} t + Z_0 \sin\theta}. \tag{3}$$

where t is the thickness of the substrate.

We design the metasurface at 9.41 GHz with the tri-layer structure using a substrate with $\epsilon_r = 2.53$ and $t = 0.8$ mm. Fig. 4 shows the capacitance or inductance values corresponding to the phase shift of θ calculated from the shunt impedances of the three layers by

$$C_u = -1/\omega\Im(Z_u) \quad (\text{when } \Im(Z_u) < 0),$$
$$L_u = \Im(Z_u)/\omega \quad (\text{when } \Im(Z_u) \geq 0). \tag{4}$$

where $u = \{\text{top}, \text{mid}, \text{bot}\}$ and ω is the angular frequency. It can be seen from the figure that any amount of the phase shift can be implemented with practically available CL values except near several particular angles where the CL values diverge. It is found that the phase shift from 0.13 rad to 3.44 rad can be realized by capacitive cells with $(C_{\text{top}}, C_{\text{bot}})$ and C_{mid} less than

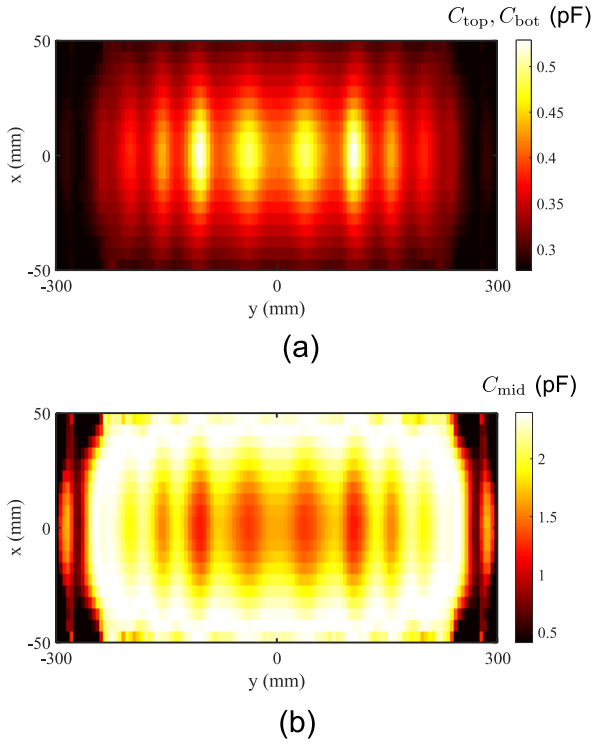

Figure 5. Capacitance distributions required to be implemented on (a) the top/bottom and (b) middle layers

1 pF and 2.4 pF, respectively (see the shaded areas in Fig. 4). This implies that the maximum cell-to-cell difference in the phase shift is 3.31 rad, which is sufficient to compensate the phase variations up to 2.88 rad in the dashed region of Fig. 2(b). The capacitance values can be implemented by interdigitated capacitors and controlled by their finger lengths [4]. Fig. 5(a) and (b) shows the capacitance distributions required to be implemented on the top/bottom and middle layers, respectively, for compensating the phase variations on the antenna aperture.

III. Numerical Simulations

In order to demonstrate the side lobe suppression by the proposed metasurface with the slot array antenna, full-wave simulations are carried out. In the simulations, the metasurface of 20×120 cells covers over the entire aperture area of the slot array antenna. Each cell is composed of two substrates of 0.8-mm thickness and three impedance boundaries with the impedances given by (3). The relative permittivity and loss tangent of the substrate are chosen to be 2.53 and 0.0018, respectively. The frequency of the incident wave is set to 9.41 GHz.

Fig. 6 shows the simulated electric-field phase distribution on the transmitted side of the metasurface. Compared to the phase distribution without the metasurface of Fig. 2(b), it is seen from the figure that the phase in the aperture is compensated by the metasurface including the aperture edge and the uniformity over the entire aperture area is improved. Fig. 7 shows the simulated radiation gain pattern of the slot array antenna. The blue and red lines are the E (*yz*) and H (*zx*) plane patterns, respectively, and solid and dashed lines are the radiation patterns with and without the metasurface, respectively. It is seen from the figure that the side lobes are significantly suppressed in both the E and H planes to be less than –24 dB. Moreover, the peak gain of the main lobe is increased by 1.4 dB compared to that without the metasurface.

IV. Conclusions

A reflectionless tri-layer metasurface that suppresses the side lobe level of the linear slot array antenna has been proposed for marine radar applications. The metasurface introduces a position-dependent phase shift in the aperture so that the phase deviations are compensated including the edge of the aperture. Due to the realized phase uniformity over the aperture, significant side lobe suppressions to be less than –24 dB with the gain enhancement of the main lobe by 1.4 dB have been achieved by the metasurface.

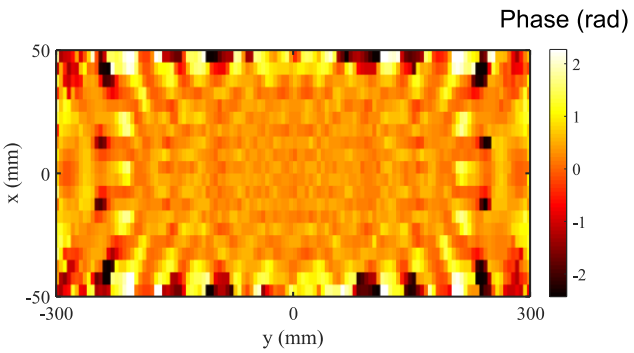

Figure 6. Electric-field phase distribution on the aperture of the antenna covered with the metasurface. Compared to Fig. 2(b), the phase uniformity over the entire aperture is improved including the aperture edge.

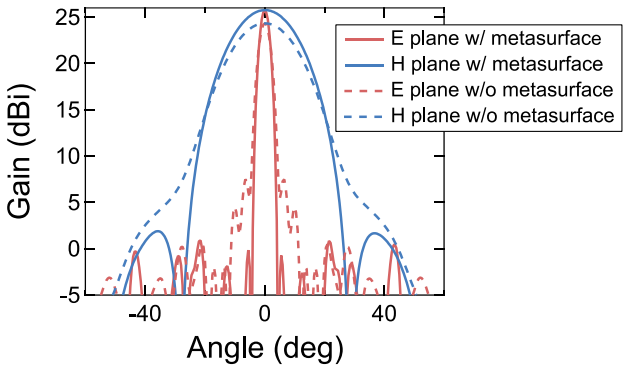

Figure 7. Simulated radiation gain pattern.

References

[1] Y. She, M. Hirose, Y. Kato, T. Ishizone, S. Kurokawa, S. Iwasawa, and S. Arata, "A Simply Structured Transverse Slot Linear Array Antenna in a Quasi-TEM Mode Waveguide," *IEICE Trans. Electron.*, vol. E100-C, no. 10, pp. 924-927, Oct. 2017.

[2] C. A. Balanis, *Antenna Theory: Analysis and Design*, New York, NY, USA: Wiley, 1997.

[3] A. Epstein and G. V. Eleftheriades, "Arbitrary Power-Conserving Field Transformations With Passive Lossless Omega-Type Bianisotropic Metasurfaces," *IEEE Trans. Antennas and Propag.*, vol. 64, no. 9, pp. 3880-3895, Sept. 2016.

[4] Y. Shigeta, A. Sanada, A. Fukuda, K. Kawai and H. Okazaki, "Reflectionless Metalens Collimating Multi-OAM Waves for Antenna Gain Enhancement in Wireless Communication," 2018 Asia-Pacific Microwave Conference (APMC), Kyoto, 2018, pp. 1205-1207.